中国光学 Chinese Optics 核心期刊

亚波长尺度下混合等离子泄漏模式激光

严闪闪 王双鹏 宿世臣

Hybrid plasmonic leaky-mode lasing on subwavelength scale

YAN Shan-shan, WANG Shuang-peng, SU Shi-chen

引用本文:
严闪闪, 王双鹏, 宿世臣. 亚波长尺度下混合等离子泄漏模式激光[J]. 中国光学, 2021, 14(2): 397−408. doi: 10.37188/CO.2020−0108
YAN Shan-shan, WANG Shuang-peng, SU Shi-chen. Hybrid plasmonic leaky-mode lasing on subwavelength scale[J]. *Chinese Optics*, 2021, 14(2): 397-408. doi: 10.37188/CO.2020-0108

在线阅读 View online: https://doi.org/10.37188/CO.2020−0108

您可能感兴趣的其他文章

Articles you may be interested in

钙钛矿材料在激光领域的研究进展
Research progress of perovskite materials in the field of lasers
中国光学. 2019, 12(5): 993 https://doi.org/10.3788/CO.20191205.0993

漫反射金膜在1.064 μm波长处的反射特性
Reflective characteristics for diffusing gold films at a wavelength of 1.064 μm
中国光学. 2019, 12(4): 913 https://doi.org/10.3788/CO.20191204.0913

激光微角偏移测试系统研究
Laser micro angular deviation measurement system
中国光学. 2017, 10(2): 234 https://doi.org/10.3788/CO.20171002.0234

基于激光的测量技术在燃烧流场诊断中的应用
Applications of measurement techniques based on lasers in combustion flow field diagnostics
中国光学. 2018, 11(4): 531 https://doi.org/10.3788/CO.20181104.0531

空气导热作用下Nd:YAG晶体温场特性
Temperature field of Nd: YAG crystal under air heat transfer
中国光学. 2019, 12(3): 686 https://doi.org/10.3788/CO.20191203.0686

用于超冷原子囚禁的一体式结构三维光晶格系统
The integrated three dimensional optical lattice system for confining ultra−cold atoms
中国光学. 2019, 12(6): 1295 https://doi.org/10.3788/CO.20191206.1295

文章编号 2095-1531(2021)02-0397-12

Hybrid plasmonic leaky-mode lasing on subwavelength scale

YAN Shan-shan[1,2], WANG Shuang-peng[2*], SU Shi-chen[1,3*]

(1. *Institute of Semiconductor Science and Technology*, *South China Normal University*, *Guangzhou* 510631, *China*;
2. *Institute of Applied Physics and Materials Engineering*, *University of Macau*, *Macau* 999078, *China*;
3. *SCNU Qingyuan Institute of Science and Technology Innovation Co.*, *Ltd.*, *Qingyuan* 511517, *China*)

* *Corresponding author*, *E-mail*: *spwang@um.edu.mo*; *shichensu@scnu.edu.cn*

Abstract: Due to the existence of diffraction limit as the basic characteristic of light, the lasing on subwavelength scale cannot be achieved by traditional methods. In order to break this diffraction limit, a stacked structure composed of metal, dielectric layer and semiconductor was designed in this paper to achieve lasing on the deep subwavelength scale and its influence on the propagation mode was discussed. In terms of structural design, we used silver, a metal with low dielectric constant, as the substrate, a 10 nm-thick LiF layer as the dielectric layer, and a ZnO semiconductor nanowire with hexagonal section as the high-dielectric-constant layer. We adopted the finite-difference eigen mode and Finite-Difference Time-Domain (FDTD) method to perform optical simulation of the designed structure. First, by changing the nanowire diameter and using the finite eigen mode, the optical modes in the dielectric layer were analyzed to obtain four mode distributions. Then the effective refractive indexes and losses of the four optical modes at different nanowire diameters were used to calculate the corresponding waveguide propagation distances and lasing threshold gains. Finally, the three-dimensional FDTD method was introduced to simulate the electric field distribution of the four modes during the steady-state laser emissionin of the nanowire. The results showed that there were hybrid plasmonic mode and hybrid electric mode in the dielectric layer between the nanowire and the metal substrate. When the diameter of ZnO nanowire was smaller than 75 nm, there was no effective physical optical mode, that is, both the hybrid plasmonic mode and the hybrid electric mode were cut off. When the nanowire diameter was larger than 75 nm, the hybrid plasmonic mode could effectively exist. The hybrid electric mode

收稿日期:2020-06-18; **修订日期**:2020-07-27

基金项目:国家自然科学基金(No. 61574063);广东省科技基金(No. 2017A050506047, No. 2017B030311013);广州市科技计划(No. 2016201604030047, No. 201804010169);广东省科技计划(No. 2019B090905005);澳门特别行政区科学技术发展基金(No. 0125/2018/A3, No. 0071/2019/AMJ);澳门大学 MYRG(No. MYRG-00149-FST)

Supported by National Natural Science Foundation of China (No. 61574063); Science and Technology Program of Guangdong Province (No. 2017A050506047, No. 2017B030311013); Guangzhou Science and Technology Project (No. 2016201604030047, No. 201804010169); Guangdong Province Scientific and Technology Project (No. 2019B090905005); Science and Technology Development Fund (No. 0125/2018/A3, No. 0071/2019/AMJ) from Macau SAR; Multi-Year Research Grants (No. MYRG-00149-FST) from University of Macau

did not appear until the nanowire diameter reached 120 nm. Although the hybrid plasmonic mode could be better confined to the dielectric layer, its loss was too large and its propagation distance was relatively small. In addition, the hybrid electric mode traveled a longer distance than hybrid plasmonic mode. At the given diameter of the micron wire (D = 240 μm), the hybrid electric mode propagated for over 50 μm. In conclusion, the hybrid leaky mode on the deep subwavelength scale can break the optical diffraction limit and realize lasing.
Key words: laser; leaky-mode; subwavelength; waveguide

亚波长尺度下混合等离子泄漏模式激光

严闪闪[1,2], 王双鹏[2*], 宿世臣[1,3*]
（1. 华南师范大学 半导体科学技术研究院，广东 510631；
2. 澳门大学 应用物理与材料工程研究所，澳门 999078；
3. 华南师大（清远）科技创新研究院有限公司，清远 511517）

摘要: 由于光存在衍射极限，因此传统方法不能实现亚波长尺度下的激光激射。为了打破这一衍射极限，本文设计了金属-介电层-半导体堆叠结构来实现深亚波长尺度下的激光激射，并讨论了相关结构对模式传播的影响。结构设计上，采用低介电常数金属银作为衬底、10 nm 厚的 LiF 作为介电层、具有六边形截面的半导体纳米线 ZnO 作为高介电常数层，采用有限差分本征模和时域有限差分方法对所设计的结构进行光学仿真模拟。首先，通过改变 ZnO 纳米线的直径，使用有限本征模方法分析介电层中的光学模式，得到 4 种模式分布。然后，通过这 4 种光学模式在不同纳米线直径下的有效折射率和损耗计算了对应的波导传输距离以及激射阈值增益。最后，采用三维时域有限差分方法仿真分析纳米线稳态激光发射过程中各模式的电场分布。结果表明：在纳米线和金属衬底之间的介电层上存在混合等离子体模式和混合电模式，对于直径低于 75 nm 的 ZnO 纳米线，没有有效的物理光学模式，即混合等离子体模式和混合电模式都被切断，当 ZnO 纳米线的直径大于 75 nm 时，混合等离子体模式可以有效存在，而混合电模式在 ZnO 纳米线的直径达到 120 nm 之后才出现。虽然混合等离子体模式可以更好地限制在介电层中，但是它们的模式损耗太大，传播距离相对较小。此外，与混合等离子体模式相比，混合电模式的传播距离更长。在给定微米线的直径 (D = 240 μm) 下，混合电模式传播距离超过 50 μm。综上可知，在深亚波长尺度下利用混合泄漏模式可以打破光学衍射极限并实现激光激射。
关　键　词: 激光；泄漏模式；亚波长；波导
中图分类号: O432.1+2; O472+.3　　**文献标志码:** A　　**doi:** 10.37188/CO.2020-0108

1 Introduction

With the continuous miniaturization and integration of modern optical devices, the diffraction limit is the major factor influencing the development of traditional optics. Surface Plasmon Polariton (SPP) is the key to break the diffraction limit for confining light within a smaller scale and to achieve smaller light spot focusing and transmission[1-3]. SPP is a special form of electromagnetic field which is localized in the metal-dielectric cross-section. It propagates along the metal surface and attenuates perpendicularly to both sides of the cross-section. Due to the surface propagation characteristics of surface plasmon wave, SPP-based metal nanostructures are capable of trapping light to subwavelength scale. The introduction of SPPs can greatly reduce the size of photonic elements and integrated light paths; therefore, it has broadened application prospects in the fields of subwavelength photonics[4-5], optical storage[6-7], microscopy[8-9] and biology[10-11].

In the past decades, lasers with small sizes have been realized, ranging from micro-sized VCSELs[12], microdisk laser[13], photonic crystal laser[14] to subwavelength plasmonic metal-based resonator

structure lasers[15-16]. The idea of implementing lasers on semiconducting nanowires with strong confinement fields has been proved particularly successful[17-18]. However, these types of laser exceed half the wavelength of the optical field in both the optical mode size and the physical device size. And it is still a challenge to realize an ultra-compact laser that can directly generate a coherent optical field at the nanometer level. The introduction of surface plasmons that can tightly confine the light field is one of the methods to solve this problem. Simultaneously acting as a gain medium and a perfect resonant cavity, the semiconductor nanowires guide modes at its end face or cross-section with reflection. For diameters smaller than half the effective wavelength of the nanowires, the transverse confinement of the modes obviously decreases. It pushes higher order modes below cutoff which leads to a reduction of the gain overlap for all modes[19]. Subwavelength scale lasers could be realized by introducing a metallic cladding around the nanowires with the principle of SPPs. The subwavelength confinement of storing optical energy in electron oscillations within metal-dielectric interface makes it possible to reduce the size of nanowire lasers[20]. Zhang's group have experimentally realized plasmon lasers at deep subwavelength scale in a structure with a semiconductor nanowire sitting on top of a metallic surface, separated by nanometer-scale insulating gap[21]. The coupling between the plasmon and the waveguide modes across the gap enables energy to be stored in non-metallic regions. The hybrid modes assist photons to travel a relatively long distance under strong mode confinement[22] and combine high-quality semiconductor gain materials with the confinement mechanism itself.

In this paper, we study the subwavelength scale leaky lasing within a system of an active ZnO nanowire separated from a metal surface by a nanoscale dielectric gap. The diameter of the plasmonic semiconductor nanowires is smaller than the wavelength of the emitted light, and there still exist bound modes that strongly overlap with the gain medium. However, the plasmonic semiconductor nanowires retain bound modes at the expense of introducing high ohmic losses in the metal. And the gain-guided Hybrid Electric (HE) mode exhibits lasing action easily than that of the bound hybrid plasmonic (HSP) mode. Next, we have performed mode calculations on plasmonic ZnO nanowires system to confirm that hybrid electric modes are more likely to realize subwavelength scale lasing, instead of hybrid plasmonic modes. First of all, we determined the modes in the cross-section of the system and obtained their respective effective refractive index and modal loss by varying the diameter of ZnO nanowire, then calculated their confinement to the gain medium and dielectric layer of the leaky modes. After comparative analyses, it was found that the hybrid electric mode arises at diameters above 120 nm and the earlier emergence of HE1 mode makes lasing much likely to generate. Finally, we demonstrated that leaky lasing occurs in the HE1 mode using finite difference time-domain method of nonlinear 3D simulations.

2 Model design and simulation method

Model design: The hybrid waveguide geometry shown in Figure 1 consists of a relatively high-permittivity semiconductor nanowire ZnO (hexagonal waveguide) placed on a low-permittivity dielectric near a metal (silver substrate) surface. In the following study, we vary the hexagonal diameter D, and fixed the spacing between the ZnO nanowire and the metal plane to study the optical parameters and electromagnetic field distribution of hybrid mode at the excitation wavelength of ZnO, i.e. λ = 380 nm. The modal dispersion and mode parameters are calculated using Finite Difference Eigenmode Solver (FDES) analysis component of MODE Solutions, where the refractive index of ZnO nanowires and dielectric layer are taken as 2.45 and

1.5, respectively. And the metallic region is silver with the permittivity of Johnson and Christy model[23].

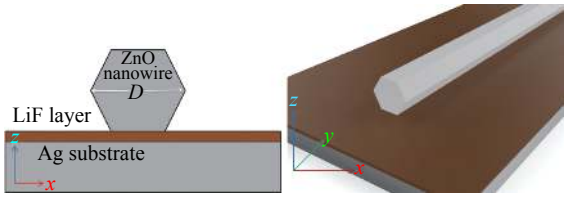

Fig. 1 A hexagonal semiconductor nanowire placed on a flat silver substrate separated by a 10 nm thin LiF layer. The upper medium is LiF layer with refractive index of 1.5 and its center defines the origin ($x = y = z = 0$).

Numerical calculations: The hybrid mode field distribution was simulated via the commercial-Lumerical's Mode Solutions of FDES. The FDES calculates the spatial profile and frequency dependence of modes by solving Maxwell's equations on a cross-section of the waveguide. The effective index is calculated with the electromagnetic wave propagation parameters. Besides, confinement factor is calculated with the energy ratio. With the real and imaginary part of effective index, the modal loss and propagation distance were determined. The extremities of the calculation region were more than half a wavelength away from the Perfect Matched Layer (PML) ensuring an open boundary condition. The diameter of the ZnO nanowires was varied to obtain the modal field distribution and calculate the corresponding parameters. In order to determine that the leaky mode lasing is indeed observed, nonlinear three-dimensional simulations in the full-time domain were performed with Lumerical's FDTD Solutions. The distribution of the lasing in the structure was simulated by using a pump light source and a four-level dual electron material model.

3 Results and discussion

For nanowires with diameter (D) below 75 nm, calculations show no effective physical optical mode. For diameters higher than 75 nm but below 120 nm, only one waveguide mode appears. In other words, HSP1 mode is the only lowest order mode that does not cut off. Interestingly, as the diameter continues to increase, HE modes and higher-order HSP modes emerge. As shown in Figure 2 (Color online), there are two waveguide modes at D = 120 nm: HSP1, HE1. An additional two waveguide modes appear at D = 200 nm show the higher-order HSP and HE modes. By comparing the two different modes, it can be clearly seen that the HSP mode confines photons better in the dielectric layer, while the HE mode could only restrict part of the photons in the dielectric layer. It can also be seen that some of the energy is confined to the ZnO nanowires. In addition, the larger diameter nanowires confined photon energy better in the HE1 and HE2 modes. These two modes also have common features in their mode distribution, as do the two other modes. All hybrid modes are confined to the separation layer between the ZnO nanowire and the metal substrate, but the HE mode extends far into the nanowire.

The energy distribution along the z-direction intuitively explains the difference between the HSP and HE modes. In this hybrid plasmon waveguide, the energy of the HSP mode is greatly enhanced in the LiF layer. The electric field distribution along the direction perpendicular to the metal substrate is shown in Figure 3(a). For the HSP1 mode, the electric field strength in the LiF layer is more than ten times that of its surroundings. This is because the electric displacement vector in the z-direction of the HSP mode is continuous, so there must be a strong local field in a region with a small dielectric constant. It can be noticed that there is a relatively strong electric field in the area between the LiF layer and the Ag substrate. This phenomenon occurs because of the surface plasmon resonance occuring at the interface. In contrast, the electric field of the HE1 mode is mainly distributed within the nanowires. To further understand the difference between the HSP and HE modes, we also compared

the field distribution of the HE1 and HSP1 modes in various directions, as shown in Figure 3(b)、3(c). It can be observed that the electric field components of HSP mode mainly occurs in the *z*-direction, which is, perpendicular to the axis of the nanowires. However, the HE mode is quite different and there are relatively strong electric field distributions in the three directions. Due to photon leakage, the two modes can limit photons in the dielectric layer. Furthermore, the leaky modes experience a second off (not shown here) and additional energy leaks into the air through the metal when the effective refractive index is close to 1.

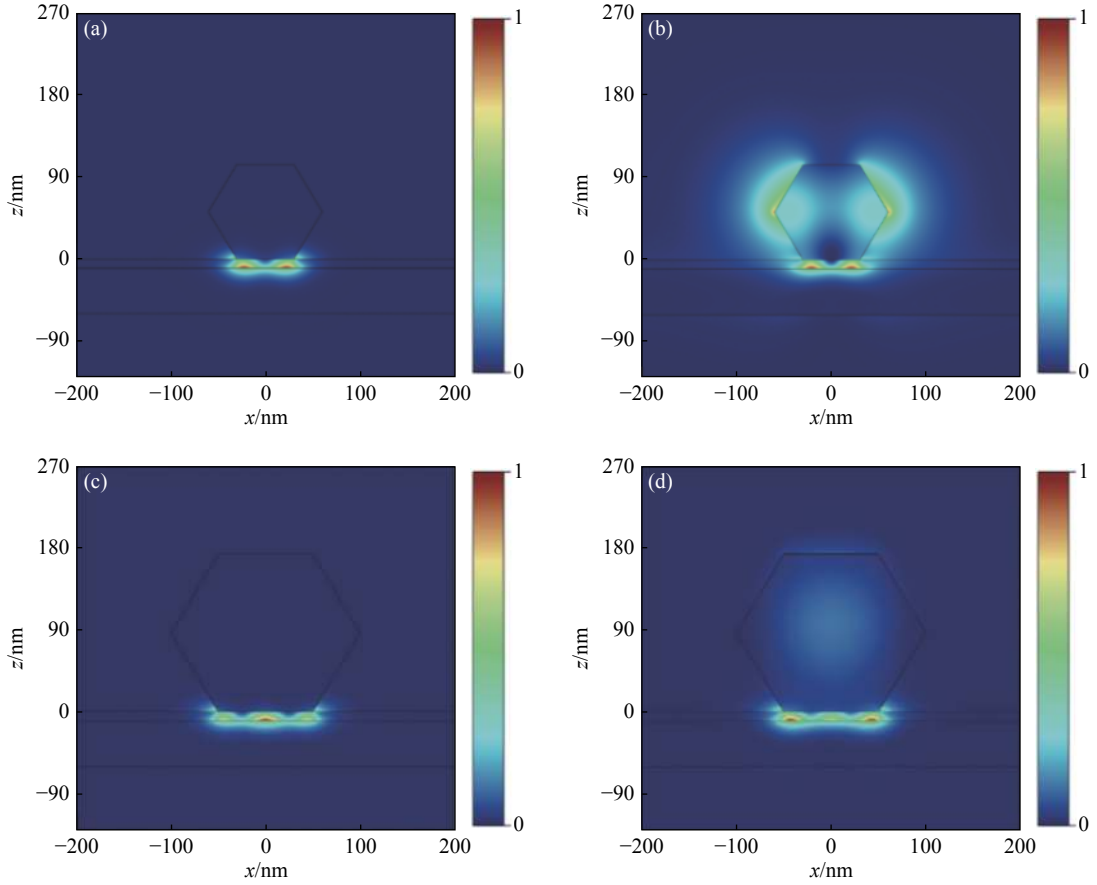

Fig. 2　Spatial electric filed distribution for the modes of (a) HSP1 and (b) HE1 at $D = 120$ nm, (c) HSP2 and (d) HE2 at $D = 200$ nm.

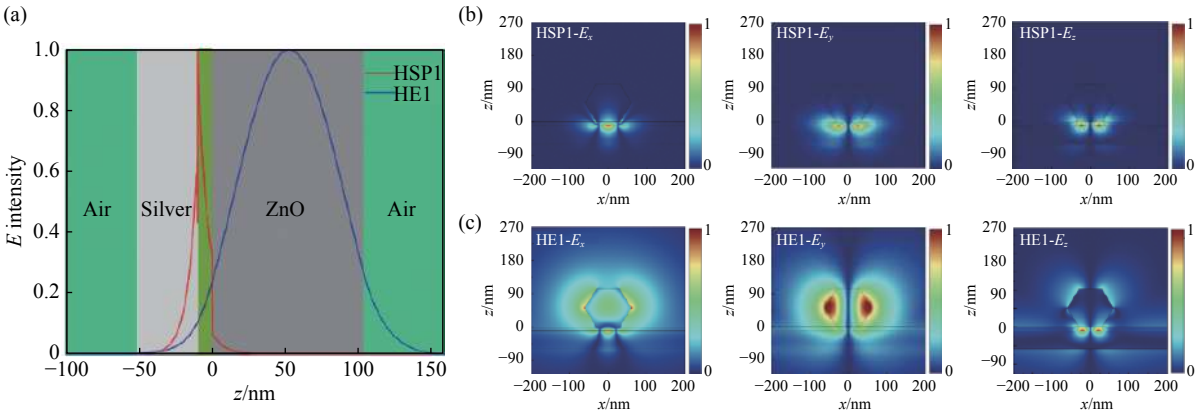

Fig. 3　(a) Energy distribution along the *z* direction of HSP1 mode and HE1 mode. The diameter of ZnO nanowire is 120 nm. Electric field components E_x, E_y, E_z of (b) HSP1 mode and (c) HE1 mode.

Figure 4 shows the effective refractive index and mode confinement factor at different ZnO diameters for each mode in the HSP and HE waveguide modes. It can be seen that the HE modes are cut off below 120 nm. Below the cutoff values, the modes leak energy into the SPPs of the Ag-LiF-Air interface, which has an effective index of n_{spp} (380 nm) ≈ 1.6. As shown in Figure 4(a), the effective refractive indexs of the HSP modes can exceed the actual refractive index of the ZnO, while the HE mode cannot. The minimum dimension requirement for a laser was obtained as follows[24]:

$$L_{min} = \lambda/2n_{eff} \quad . \tag{1}$$

L_{min} is the well-known half-wavelength condition or diffraction limit associated with any wave. The large effective refractive index of the HSP mode is very important for reducing the length of the laser. It is worth noting that the four modes simultaneously appear at a nanowire diameter of 170 nm. On this basis, the HSP1 mode is converted to HSP2 mode with the increase in diameter. Interestingly, HE2 mode appears earlier than the HSP2 mode. This mode switching is due to the interaction between material dispersion in the metal and modal dispersion, which is due to the mode confined to the nanowire. In the case of large diameters, the effect of the metal substrate on the HE modes converges to a common effective refractive index: close to a purely dielectric ZnO nanowire.

The other minimum length requirement has to be at least long enough to overcome a threshold loss determined by the facet reflectivity, which is directly proportional to reflectivity and inversely proportional to the given mode gain, G_{mode}. The modal gain, which is typically defined as material gain G_0, times the so-called confinement factor Γ, determines the amplification rate of the power of a given mode[24]:

$$G_{mode} = \Gamma G_0 \quad , \tag{2}$$

where Γ is the confinement factor of the gain medium region, which dominates the interaction strength of the modal field with the gain material. This is a convenient relationship because it decomposes the modal gain into the pure material properties (material gain) and pure geometric properties of the waveguide.

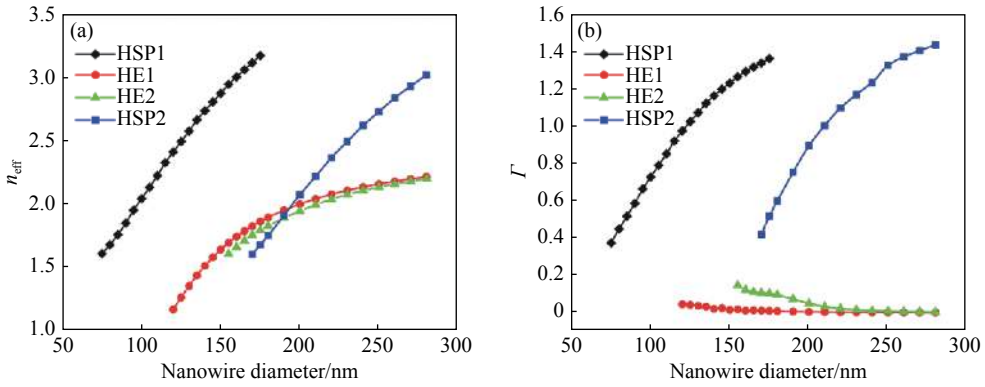

Fig. 4 (a) Effective refractive index and (b) mode confinement factor at different diameters for each mode in HSP and HE waveguide modes.

Since the optical mode confined to the dielectric layer is essential, the confinement factor of the LiF layer is shown in Figure 4(b). It could be observed that the Γ of the HSP modes can take values larger than those in strongly guiding systems. However, since the dielectric layer is in direct contact with the metal, the energy limit is enhanced under SPP conditions so that the confinement factor can exceed one. It was found that giant modal gain could be realized in plasmonic systems[25-26]. By increasing the diameter of the nanowire, the confinement factor of the HSP mode increases and the HE mode decreases. Now, according to Eq.(2), it is impossible in principle to achieve lasing below the

mode at the cutoff frequency because the modal gain will be zero. Here, in the case of a plasmonic ZnO nanowire laser, however, the conjecture that leakage cannot lase shall prove to be incorrect, because the confinement of the leaky mode strongly depends on the gain of the ZnO nanowire.

The modal loss coefficient and propagation distance are shown in Figure 5. The loss coefficients of the HSP modes are high for the given nanowire diameters, ranging from 4.6×10^5 dB/cm for HSP1 to 5.1×10^5 dB/cm for HSP2. The reason for the high modal loss is due to the very strong localization of the plasmonic modes to the thin separation layer and the relatively strong evanescent waves' tail entering into the metal causing ohmic loss. The loss coefficient of the SPP (α_{spp}) is about 2.2×10^4 dB/cm for HSP1. On the other hand, the HE mode have a low loss coefficient of order 1×10^3 dB/cm at large diameters, which increases for smaller diameters because of a rising overlap with the metal. It should be noted that the modal loss of the HE mode decreases with a rising diameter. When the loss coefficient exceeds its α_{spp}, the corresponding HE mode loses its confinement in space and its field grows exponentially toward the nanowire at infinity.

Evidently, the dielectric layer provides means to store electromagnetic energy, leading to sub-wavelength optical guiding with low mode loss. The propagation distances for the hybrid modes at different diameters were calculated and shown in Figure 5(b). The HSP modes have a small propagation distance of only a few micrometers, which is higher than the propagation distance of the conventional plasmonic mode. It shows that the HSP modes have characteristics of relatively low loss like the dielectric mode, and at the same time, it has the advantages of field enhancement with the surface plasmon mode. In addition, the HE mode propagates longer distances compared with the HSP mode. With the given diameter, the HE1 mode's propagations surpass 50 μm at D = 240 nm. It can be seen that the propagation distance of the HE1 mode is larger than that of the HE2 mode. When the diameter exceeds 240 nm, the propagation distance of HE1 is dramatically reduced. The reason for the decreasing propagation distance is that the photons are gradually confined to larger diameter nanowires, and the energy that leaks out into the dielectric layer is reduced.

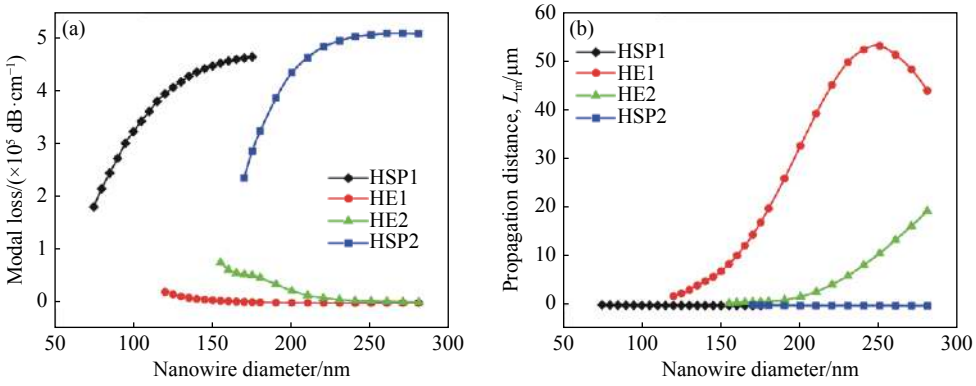

Fig. 5 (a) Modal loss coefficient α and (b) propagation distance L_m, at different diameters for each mode in HSP and HE waveguide modes.

Now, we assume that a spatially homogenous gain is introduced in the ZnO nanowire at $\varepsilon_{r,a} \approx n_a^2 + i\cdot g n_a \lambda/(2\pi)$, the modal loss will decrease accordingly by $\alpha_{eff} = \alpha_{prop} + \alpha_{leak} - (\Gamma v_{g,a}/v_E)g$[19]. Before that, by dividing the overall intensity into a leaky part and another part of the mode, we can rewrite the confinement factor Γ of the mode below the cutoff as a relation of a gain-independent factor Γ_{mode} and gain-dependent factor. The definition of Γ_{mode} is as follows:

$$\Gamma \approx \Gamma_{\text{mode}} \Big/ \left(1+\frac{\alpha_{\text{leak}}\sqrt{n_{\text{spp}}^2-n_{\text{eff}}^2}}{n_{\text{spp}}\alpha_{\text{spp}}-n_{\text{eff}}\alpha_{\text{eff}}}\right) . \quad (3)$$

The above relationship is valid for $n_{\text{spp}}\alpha_{\text{spp}}-n_{\text{eff}}\alpha_{\text{eff}}>0$, taking the mode and its evanescent fields into account. With this equation, the leaky mode will change nonlinearly since the confinement itself is gain dependent. Interestingly, the leaky modes differ from their bound modes whose confinement factor is almost independent on the gain medium. When the intensity reaches its threshold ($\alpha_{\text{eff}}=0$), the confinement factor of leaky modes is given by

$$\Gamma(g_{\text{th}}) \approx \Gamma_{\text{mode}} \Big/ \left(1+\frac{\alpha_{\text{leak}}\sqrt{n_{\text{spp}}^2-n_{\text{eff}}^2}}{(n_{\text{spp}}\alpha_{\text{spp}})}\right) . \quad (4)$$

Thus, the leaky modes can theoretically reach its lasing threshold like conventional bound modes with the threshold gain value $g_{\text{th}}=\alpha_{\text{eff}}(g_{\text{th}})/\Gamma_{\text{eff}}(g_{\text{th}})$.

The combined effect of confinement and slow energy velocity on the modal gain is shown in Figure 6(a) (Color online) in terms of the confinement factor Γ at threshold, where gain compensates for propagation loss. Compared with Figure 4(b), the confinement factor of leaky modes with modal gain presents a very good approximation to that with no modal gain. The slight differences of the previous values to the actual threshold gain above the cutoff arise from changes in the modes' profiles when the gain is introduced into the ZnO oxide, which either pulls the modal fields closer to the nanowire or pushes them out of it. Due to the values of the loss and confinement factor, the threshold gain values of the leaky modes are shown in Figure 6(b) (Color online). The leaky HSP mode and leaky HE2 mode behave with a lower threshold gain. In contrast, the threshold gain of the leaky HE1 mode dramatically increases for a large range of nanowire diameters. Below a nanowire diameter of 120 nm, the mode leaks into free-space radiation and at this point its leakage behavior is comparable to that of leaky photonic modes. When the diameter exceeds 210 nm, the cavity size of the ZnO can gradually confine the photon, resulting in a decrease of leaked energy. Above all, it would be HE1 that is most likely to cross the lasing threshold, which is also a leaky mode.

In order to determine that the leaky mode lasing is indeed observed, we perform nonlinear three-dimensional simulations in the full-time domain. The gain in the ZnO semiconductor nanowire is described via the Finite-Difference Time-Domain (FDTD) computational model of the lasing dynamics of a four-level two-electron atomic system[27]. The approach did not include the pumping dynamics or the Pauli exclusion principle. Transitions between the energy levels are governed by coupled rate equations and the Pauli exclusion principle. The wavelength of the pump source is set to be 266 nm with FWHM of 0.7 nm. The spatially uniform pump rate above the threshold power is used to create population inversion to feedback energy into the lasing system continuously. The center wavelength of the lasing is 380 nm with FWHM 0.5 nm when the system evolves into its most stable state. Since the size of the ZnO nanowire is not sufficient to trap the photons excited from the four-level and two-electron system so that most of the photons leak into the surrounding air and the dielectric layer. However, photons are blocked by metal and are confined in the dielectric layer. In the cross-sectional direction, different waveguide modes will occur for large-diameter nanowires. In the vertical direction, the lasing mode emitted by Fabry-Perot resonance along the z-direction can be a single mode in a short nanowire, and multi modes will be generated in longer nanowires. The calculation process uses Perfect Matched Layer (PML) boundary conditions that perfectly absorb electromagnetic field leaked to the boundary without affecting the field distribution of the system.

Figure 7 shows the electric field distribution for the HE1 lasing mode during steady-state lasing at D = 170 nm. The local distribution of the energy in the dielectric layer can be clearly observed. The

leaky energy of the active ZnO nanowire was effectively confined into the LiF gap during the transmission process, shown in Fig. 7(a)~7(b). Fig. 7(c) shows the electric field distribution of dielectric layer, and the mode is exactly the same as the HE1 mode obtained above. Since the emitted light from ZnO nanowire leaked into propagating SPPs and was confined in the dielectric layer. Thus, leaky mode lasing in the subwavelength scale was realized.

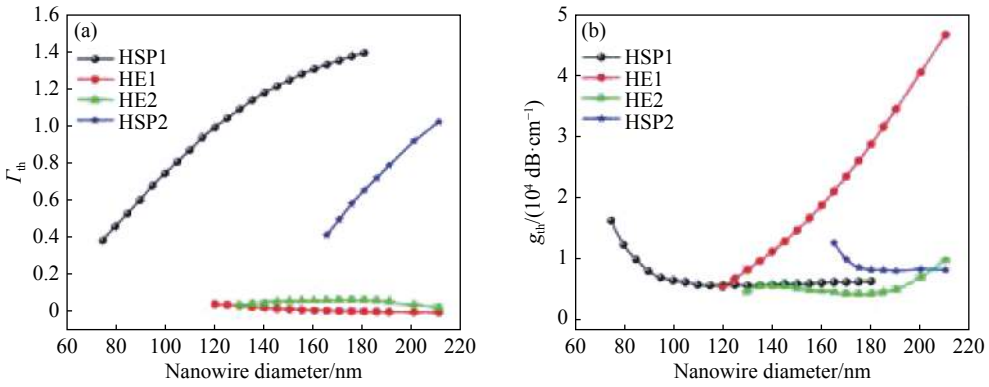

Fig. 6　(a) Confinement factor at threshold Γ_{th} and (b) threshold gain g_{th} of the hybrid modes at λ = 380 nm, the values were calculated with $g_{th} = \alpha_{eff} / \Gamma_{eff}$.

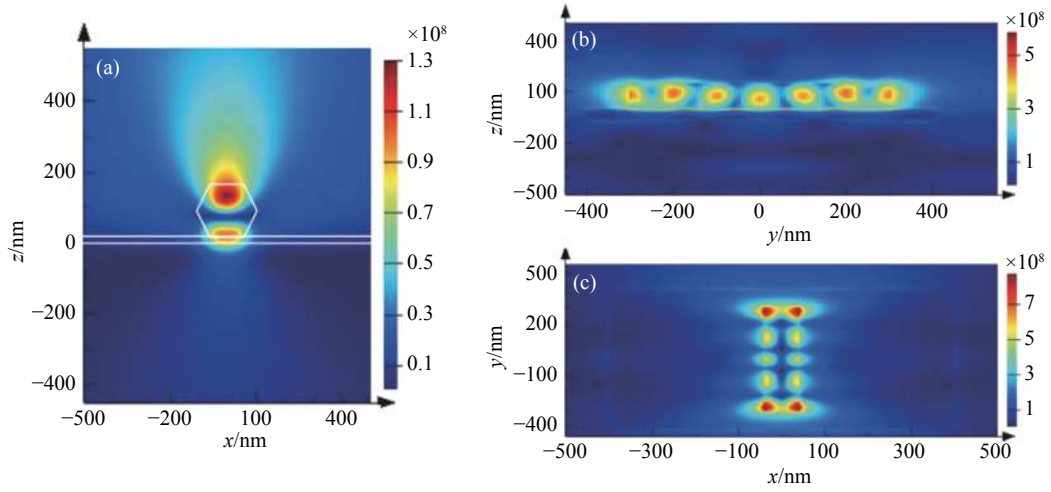

Fig. 7　Snapshots of the HE1 lasing mode electric field intensity distribution in three different section directions. (a) *xz* plane and (b) *yz* plane of the cross section of the nanowire-dielectric-metal interface; (c) *xy* plane inside the dielectric layer (z = 0). The diameter of the ZnO nanowire in the above simulation was set to be 170 nm.

4　Conclusion

In conclusion, we have proposed an approach for realizing hybrid leaky-mode lasing in a deep subwavelength scale. By varying the diameter of ZnO nanowires, there exists hybrid plasmonic modes and hybrid electric modes across the gap dielectric layer between nanowires and metal substrate. For diameters below 75 nm, there are no effective physical optical modes, that is, both HSP modes and HE modes are cutoff. In addition, the HE modes remain cutoff until the diameter of the ZnO nanowires reaches 120 nm. Although, the HSP mode could be better confined to the dielectric layer, their modal loss is too large to result in a relatively small propagation distance. Thus, hybrid electric modes are more likely to achieve leaky-mode lasing. Since the diameter of the nanowires is greater than the wavelength of the emitted light, photons are

confined well to the nanowires, resulting in a reduction in energy that is leaked. Compared to HE mode, the HE1 mode of longer propagating distance is more likely to achieve subwavelength scale lasing. Finally, the lasing action of the HE1 mode was proven by nonlinear three-dimensional simulations in the full-time domain.

Definition of optical parameters

The modal effective index is defined as[28]:

$$n_{\text{eff}} = \frac{c\beta}{\omega} \quad , \qquad (5)$$

where ω is the angular frequency and β is the propagation constant.

Mode loss is calculated based on the imaginary part of the effective index:

$$Loss(dB/m) = \frac{10n_i 4\pi}{\lambda_0 \ln 10} \quad , \qquad (6)$$

where n_i is the imaginary part of the effective index and λ_0 is the calculated center wavelength.

The propagation distance of a given waveguide mode is defined as[29]:

$$L_{\min} = [2\text{Im}\,(k)]^{-1} \quad , \qquad (7)$$

where k is the complex-mode wave vector component in the propagation direction:

$$k = n_{\text{eff}} \frac{2\pi}{\lambda} \quad . \qquad (8)$$

Since increasing confinement factor Γ can help in the miniaturization of the laser system. The Γ is introduced as a measure of the fraction of the material gain that amplifies a given mode, as expressed in Eq. (2). Confinement factor is defined as[24]:

$$\Gamma = \frac{2\varepsilon_0 c n_b \iint \mathrm{d}x\mathrm{d}y |\boldsymbol{E}|^2_{\text{active}}}{\iint \mathrm{d}x\mathrm{d}y [\boldsymbol{E}\times\boldsymbol{H}^* + \boldsymbol{H}\times\boldsymbol{E}^*]\cdot\hat{z}} \quad , \qquad (9)$$

where ε_0 is dielectric constant of vacuum, c is the speed of light in vacuum and n_b is the background refractive index. It is worth noting that the integral region in the molecule is limited to the active region, while the integral region in the denominator is the cross-section of the entire waveguide.

参考文献:

[1] RUST M J, BATES M, ZHUANG X W. Sub-diffraction-limit imaging by stochastic optical reconstruction microscopy (STORM)[J]. *Nature Methods*, 2006, 3(10): 793-796.

[2] MAIER S A, KIK P G, ATWATER H A, *et al*.. Local detection of electromagnetic energy transport below the diffraction limit in metal nanoparticle plasmon waveguides[J]. *Nature Materials*, 2003, 2(4): 229-232.

[3] GRAMOTNEV D K, BOZHEVOLNYI S I. Plasmonics beyond the diffraction limit[J]. *Nature Photonics*, 2010, 4(2): 83-91.

[4] BARNES W L, DEREUX A, EBBESEN T W. Surface plasmon subwavelength optics[J]. *Nature*, 2003, 424(6950): 824-830.

[5] BOZHEVOLNYI S I, VOLKOV V S, DEVAUX E, *et al*.. Channel plasmon subwavelength waveguide components including interferometers and ring resonators[J]. *Nature*, 2006, 440(7083): 508-511.

[6] PARK S, HAHN J W. Plasmonic data storage medium with metallic nano-aperture array embedded in dielectric material[J]. *Optics Express*, 2009, 17(22): 20203-20210.

[7] MANSURIPUR M, ZAKHARIAN A R, LESUFFLEUR A, *et al*.. Plasmonic nano-structures for optical data storage[J]. *Optics Express*, 2009, 17(16): 14001-14014.

[8] KUBO A, PONTIUS N, PETEK H. Femtosecond microscopy of surface plasmon polariton wave packet evolution at the silver/vacuum interface[J]. *Nano Letters*, 2007, 7(2): 470-475.

[9] SMOLYANINOV I I, ELLIOTT J, ZAYATS A V, *et al*.. Far-field optical microscopy with a nanometer-scale resolution based on the in-plane image magnification by surface plasmon polaritons[J]. *Physical Review Letters*, 2005, 94(5): 057401.

[10] NELSON B P, GRIMSRUD T E, LILES M R, *et al*.. Surface plasmon resonance imaging measurements of DNA and

RNA hybridization adsorption onto DNA microarrays[J]. *Analytical Chemistry*, 2001, 73(1): 1-7.

[11] SMITH E A, THOMAS W D, KIESSLING L L, *et al*.. Surface plasmon resonance imaging studies of protein-carbohydrate interactions[J]. *Journal of the American Chemical Society*, 2003, 125(20): 6140-6148.

[12] LEE Y H, JEWELL J L, SCHERER A, *et al*.. Room-temperature continuous-wave vertical-cavity single-quantum-well microlaser diodes[J]. *Electronics Letters*, 1989, 25(20): 1377-1378.

[13] LEVI A F J, SLUSHER R E, MCCALL S L, *et al*.. Room temperature operation of microdisc lasers with submilliamp threshold current[J]. *Electronics Letters*, 1992, 28(11): 1010-1012.

[14] PAINTER O, LEE R K, SCHERER A, *et al*.. Two-dimensional photonic band-gap defect mode laser[J]. *Science*, 1999, 284(5421): 1819-1821.

[15] MA R M, OULTON R F, SORGER V J, *et al*.. Room-temperature sub-diffraction-limited plasmon laser by total internal reflection[J]. *Nature Materials*, 2011, 10(2): 110-113.

[16] TREDICUCCI A, GMACHL C, CAPASSO F, *et al*.. Single-mode surface-plasmon laser[J]. *Applied Physics Letters*, 2000, 76(16): 2164-2166.

[17] CHU SH, WANG G P, ZHOU W, *et al*.. Electrically pumped waveguide lasing from ZnO nanowires[J]. *Nature Nanotechnology*, 2011, 6(8): 506-510.

[18] JOHNSON J C, CHOI H J, KNUTSEN K P, *et al*.. Single gallium nitride nanowire lasers[J]. *Nature Materials*, 2002, 1(2): 106-110.

[19] WUESTNER S, HAMM J M, PUSCH A, *et al*.. Plasmonic leaky-mode lasing in active semiconductor nanowires[J]. *Laser & Photonics Reviews*, 2015, 9(2): 256-262.

[20] NEZHAD M P, SIMIC A, BONDARENKO O, *et al*.. Room-temperature subwavelength metallo-dielectric lasers[J]. *Nature Photonics*, 2010, 4(6): 395-399.

[21] OULTON R F, SORGER V J, ZENTGRAF T, *et al*.. Plasmon lasers at deep subwavelength scale[J]. *Nature*, 2009, 461(7264): 629-632.

[22] OULTON R F, BARTAL G, PILE D F P, *et al*.. Confinement and propagation characteristics of subwavelength plasmonic modes[J]. *New Journal of Physics*, 2008, 10(10): 105018.

[23] JOHNSON P B, CHRISTY R W. Optical constants of the noble metals[J]. *Physical Review B*, 1972, 6(12): 4370.

[24] NING C Z. Semiconductor nanolasers[J]. *Physica Status Solidi* (*B*): *Basic Solid State Physics*, 2010, 247(4): 774-788.

[25] LI D B, NING C ZH. Peculiar features of confinement factors in a metal-semiconductor waveguide[J]. *Applied Physics Letters*, 2010, 96(18): 181109.

[26] LI D B, NING C ZH. Giant modal gain, amplified surface plasmon-polariton propagation, and slowing down of energy velocity in a metal-semiconductor-metal structure[J]. *Physical Review B*, 2009, 80(15): 153304.

[27] CHANG S H, TAFLOVE A. Finite-difference time-domain model of lasing action in a four-level two-electron atomic system[J]. *Optics Express*, 2004, 12(16): 3827-3833.

[28] ZHU ZH M, BROWN T G. Full-vectorial finite-difference analysis of microstructured optical fibers[J]. *Optics Express*, 2002, 10(17): 853-864.

[29] OULTON R F, SORGER V J, GENOV D A, *et al*.. A hybrid plasmonic waveguide for subwavelength confinement and long-range propagation[J]. *Nature Photonics*, 2008, 2(8): 496-500.

Author Biographics：

YAN Shan-shan (1993—), male, born in Huangshi, Hubei, PhD candidate. He received his BS degree from Hubei University, and his MS degrees from South China Normal University in 2015 and 2018, respectively, all in Electrical Engineering. Shanshan Yan's research interest has been in the area of traditional wide bandgap semiconductor and the latest perovskite materials. E-mail: yb87810@um.edu.mo

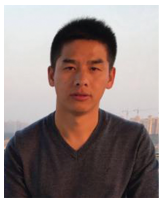

SU Shi-chen (1980 —) male, born in Jiamusi, Heilongjiang. Dr. Su received his doctoral degree in science from Changchun Institute of Optics, Fine Mechanics and Physics, Chinese Academy of Sciences in 2009. He is now a professor in South China Normal University. He is engaged in the research of wide bandgap semiconductor materials, such as ZnO and GaN, as well as their applications in optoelectronics. E-mail: shichensu@scnu.edu.cn

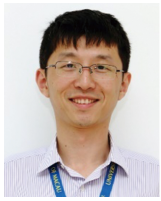

WANG Shuang-peng (1982 —) male, born in Harbin, Heilongjiang. Dr. Wang is an assistant professor in IAPME at University of Macau. He got his doctorate from Changchun Institute of Optics, Fine Mechanics and Physics, Chinese Academy of Sciences in 2011. His research interests are group II oxide, low dimensional materials and their optoelectronic application. E-mail: spwang@um.edu.mo